Fine-Tuning of Superhydrophobicity Based on Monolayers of Well-defined Raspberry Nanoparticles with Variable Dual-roughness Size and Ratio

Camille C. M. C. Carcouët, A. Catarina C. Esteves, Marco M. R. M. Hendrix, Rolf A. T. M. van Benthem, and Gijsbertus de With**

Superhydrophobic surfaces have been extensively investigated for self-cleaning, low-adhesion, anti-corrosion or reduced-drag applications. Roughness and its characteristics, i.e., morphology, overall roughness and individual feature size, is an essential factor for superhydrophobicity. Several experimental methods and theoretical models strived to predict how the surface wettability is affected by the surface roughness. However, due to the difficulty of making practical surfaces with well-defined roughness profiles, only limited and arbitrary experimental studies focused on practical superhydrophobic films. Here, the roughness factors which determine the wetting properties of films are reported, based on monolayers of well-defined raspberry silica-silica nanoparticles, exhibiting a wide-range and systematic variation of individual features sizes and ratios (large over small features). The advancing water contact angle does not depend on the feature size or ratio, while the contact angle hysteresis (CAH) is strongly dependent on both. The minimum size and size ratio to reach superhydrophobicity were determined. These new insights into the wetting of rough surfaces can be used to direct the design of practical superhydrophobic materials for advanced applications such as solar panels, microelectronics or microfluidic devices.

1. Introduction

Over the last decade, superhydrophobic surfaces have attracted much interest from both a fundamental research and practical application point of view, mostly driven by the promise of self-cleaning and low-adhesion properties. The applications of superhydrophobic coatings are widely ranging, from solar panels, green-houses, sky-scrapers, airplanes, boats, clothes, microfluidics, mobile phones to electronic devices and have been adequately reviewed several times.[1–4] Research has revealed that the self-cleaning ability of the Lotus leaf originates from a peculiar topology based on micro- and nanoscopic surface roughness combined with the hydrophobic properties of its epicuticular wax.[5,6] Considerable efforts focused on the development of superhydrophobic surfaces through the design of proper roughness. Various approaches, based on etching, chemical deposition, use of colloidal particles or templates, have been reported.[7–9] Although a great deal of attention has been devoted to the development of new procedures for superhydrophobic surfaces, more fundamental knowledge on the size and scale dependency of the wetting process is still required. While theoretical models explored the role and effects of multi-scale roughness on hydrophobicity,[10,11] experimental[12,13] and theoretical[14,15] studies revealed that a double-scale roughness is primordial in creating a superhydrophobic surface. However, up to date, only a limited amount of experimental studies focusing on the fundamentals of wetting properties have been reported.[7,13,16]

Dr A. C. C. Esteves
Laboratory of Materials and Interface Chemistry
Eindhoven University of Technology
Den Dolech 2, P.O. Box 513, 5600 MB, Eindhoven, The Netherlands
E-mail: a.c.c.esteves@tue.nl
Prof. G. de With
Laboratory of Materials and Interface Chemistry
Eindhoven University of Technology
Den Dolech 2, P.O. Box 513, 5600 MB, Eindhoven, The Netherlands
E-mail: g.dewith@tue.nl
C. C. M. C. Carcouët
Laboratory of Materials and Interface Chemistry
Eindhoven University of Technology
Den Dolech 2, P.O. Box 513, 5600 MB, Eindhoven, The Netherlands
M. M. R. M. Hendrix
Laboratory of Materials and Interface Chemistry
Eindhoven University of Technology
Den Dolech, 2, P.O. Box 513,
5600, MB, Eindhoven, The Netherlands
Prof. R. A. T. M. van Benthem
Laboratory of Materials and Interface Chemistry
Eindhoven University of Technology
Den Dolech 2, P.O. Box 513, 5600, MB, Eindhoven, The Netherlands
Prof. R. A. T. M. van Benthem
DSM Ahead Performance Materials,B.V.
P.O. Box 18, 6160 MD, Geleen, The Netherlands

DOI: 10.1002/adfm.201400111

The use of raspberry particles – large spherical particles decorated with smaller spherical ones, in a raspberry-like morphology – for the preparation of superhydrophobic surfaces has been reported, mainly using silica-silica[17–19] or silica-polymer[20–23] raspberry compositions. The resulting morphology offers, if properly controlled, well-ordered hierarchical structures which consist of the ideal practical 'models' to study the wettability of superhydrophobic surfaces. For this matter, the sizes of the individual particles composing the raspberry (small and large roughness features) as well as the ratio between them, are critical factors to achieve a high water Contact Angle (CA) and a low Contact Angle Hysteresis (CAH), i.e., superhydrophobic properties. Several authors have addressed these scale and size ratio effects on raspberry originated films but in a rather arbitrary way. Lee et al.[19] investigated the surface performance of films prepared from silica-silica raspberry particles, using Layer-by-Layer (*LBL*) deposition, with varying small feature sizes (SS) from 20 to 90 nm and a constant large feature size (LS) of 500 nm, corresponding to size ratios (r = LS/SS) from 25 to 6, respectively. The hysteresis of these films was strongly related to the presence and size of the SS features and a low CAH could only be achieved for SS features below 35 nm, i.e., $r \geq 14$. Liu et al.[20] prepared superhydrophobic films from polymer-silica raspberries, using poly(styrene) (PS) particles enriched with poly(acrylic acid) chains which template the growth of small silica particles with different sizes; SS (silica) varying from 36 to 125 nm and LS (PS) having a constant size of ~300 nm. In this case, only the larger size ratios (r varied between 2 and 8) revealed improved superhydrophobic properties. In a different approach, He et al.[24] prepared films from silica-silica raspberries, using a *LBL* method mediated by polyelectrolytes, varying the large feature sizes, LS from 70 to 200 nm, while the SS features were kept constant at 20 nm, with r varying from 4 to 10. Within these size-variations, fine raspberry structures could only be achieved with $r \geq 10$, but no investigation was made on the potential superhydrophobic properties of these films, since they were aiming for anti-reflective, anti-fogging superhydrophilic surfaces. Hence, a more in depth and consistent study on the effect of the features size and size ratio on the performance of superhydrophobic surfaces is still required to understand the fundamental roles of the multi-scale roughness involved in surface wettability.

Here, we report a comprehensive and systematic study of the roughness factors which determine the wetting properties of films originated from monolayers built up with well-defined raspberry silica-silica particles, exhibiting a wide-range of individual feature sizes and sizes-ratio. The crucial element in introducing tuneable dual-size roughness in the films is the synthesis of well-defined raspberry particles. Their precise morphology offers a methodical variation of the overall raspberry particle size, as well as the size ratio (r) between large (LS) and small (SS) features comprising the raspberry.

2. Well-defined Silica-silica Raspberry Nanoparticles and Their Assembly Into Monolayers

In order to build up a matrix of raspberry particles with different sizes, well-defined and monodisperse silica particles were prepared with diameter varying from 10 to 400 nm. For sizes above 50 nm, the well-known Stöber[25] method in alcohol-based medium was used, while for sub-50 nm particles, an amino-acid based method,[26] i.e., using lysine in aqueous medium, appeared to be more successful to obtain the well-defined particles, i.e., with controlled size, polydispersity and morphology. The synthesized particles were surface modified with different chemical groups to be able to react covalently with each other and form the raspberry morphology. The smaller particles (SS) were modified with terminal amino-groups and the larger (LS) with terminal epoxy-groups (**Figure 1**a). The raspberry particles were prepared upon reaction of these modified particles in solution (see SI, experimental). By combining 4 sizes of LS particles, i.e., 130, 260, 315, and 400 nm in diameter, with 3 sizes of SS particles, i.e., 15, 25, and 45 nm, the overall size and size ratio (r) of the raspberry particles were varied in a systematic way and a matrix of raspberry silica-silica particles became available, see **Table 1** and **Figure 2**.

The films were prepared following the procedure described by Ming et al.[17] where the raspberry particles, containing primary amine groups at the SS particles, were deposited by spin coating on a pre-reacted glycidyl epoxy-amine layer prepared with 10% excess glycidyl epoxy (Figure 1d). The layer of raspberry particles is then finally covered with a monolayer of epoxy-terminated polydimethylsiloxane (PDMS) to provide for the low-surface energy. The morphology of the films produced was characterized by Scanning Electron Microscopy (SEM)

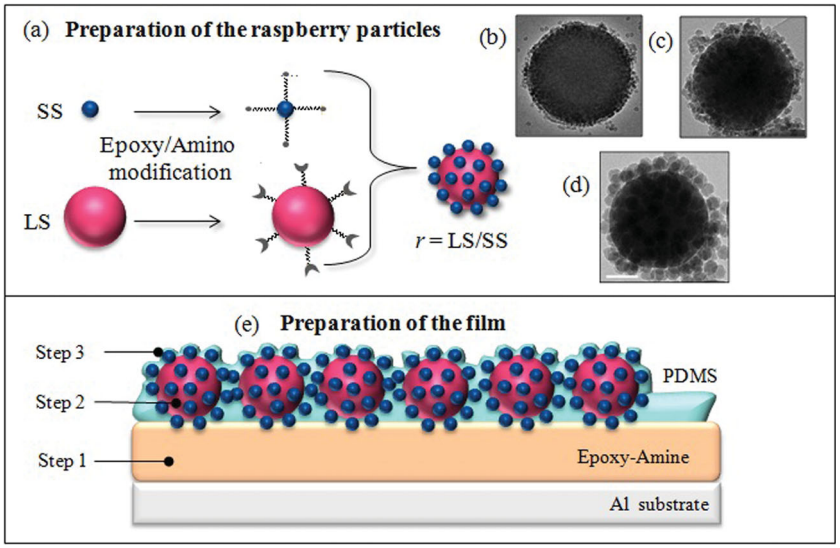

Figure 1. Schematic representation of the preparation procedure of raspberry particles (a) and representative TEM images of raspberry particles with 315/15 nm (b), 315/25 nm (c) and 315/45 nm (d) sizes (Scale bars: 100 nm). Schematic representation of the preparation procedure of the films (e) with the formation of the bonding-epoxy amine layer (Step 1), the deposition of the raspberry particles by spin-coating (Step 2) and the coverage of the surface structure with a chemically bonded PDMS thin layer (Step 3).

Table 1. Sizes of the individual large (LS) and small (SS) silica particles and size ratios of raspberry silica-silica particles (in nm).

LS →	130	260	315	400
SS ↓				
15	89	17	21	27
25	5	10	13	16
45	3	6	7	9

(see Figure 2). For all the size ratios, the films were essentially homogeneous and formed by a monolayer of raspberry particles over a large length scale with only a few small areas uncovered, showing a good level of control over the deposition of the raspberry particles and the high efficiency of the preparation method used. Note that although for larger feature sizes we have less control over the deposition process, most of the coatings are in fact monolayers.

The coatings discussed here are expected to be reasonably robust, as assessed by previous work using the pull-off test on similarly structured monolayers with reinforced necks between the small and large particles.[27] It was shown that upon full cross-linking of the epoxy-amine layer, which serves as support to the particles monolayer, the coatings become extremely robust. After pull-off test the silica particles remained attached to the epoxy-layer and no damage was observed. When a non cured epoxy-amine layer was used, all the particles were removed (see Figure SI-1).[27] For coatings with raspberry particles, made by a layer-by-layer deposition approach, an extra step of chemical bonding with $SiCl_4$ treatment was needed to maintain the small silica particles attached, and retain the raspberry like morphology (see Figure SI-2).[27] In the coatings reported here, the supporting epoxy-amine layer was fully cured. The extra $SiCl_4$ treatment was not applied because we were not mainly concerned with the robustness of the coatings. It should also be noted that in the current case, the coatings were made by the raspberry approach, i.e., directly depositing the raspberry particles which were previously formed and covalently bonded, into the epoxy–amine layer. Hence, the robustness of the coatings reported in this study may be further enhanced by a simple treatment with $SiCl_4$.

3. Wettability of Films Made from Raspberry Particles with Various Features Size and Size Ratios

The hydrophobicity of the films was characterized by measuring the advancing and receding contact angles (CA) formed by a water droplet on the surface. As a reference, the wetting properties of a PDMS film and PDMS modified single-scale films, prepared with large silica particles (LS) only, were determined (**Figure 3**a). Although a high advancing water contact angle was measured for the single-scale films (up to 151° ± 2°), the CAH was also rather high, up to 60°. Nevertheless, the water CA appeared to be independent of the size of the large particles used. Similar results were reported by Lee et al.[19] for

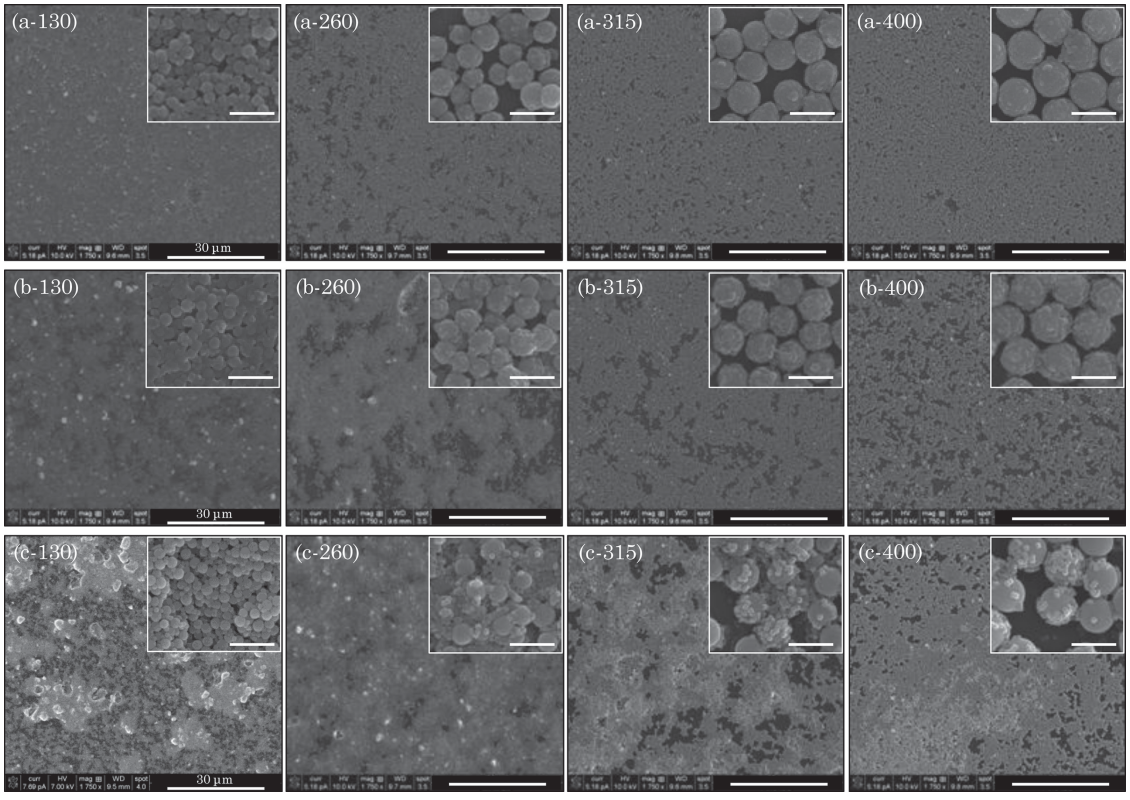

Figure 2. SEM images of the PDMS-covered films made of raspberry particles prepared with (a) 15 nm, (b) 25 nm and (c) 45 nm diameter particles as small features (see Table 1 for nomenclature details). Scale bars: 30 µm, insets: 500 nm.

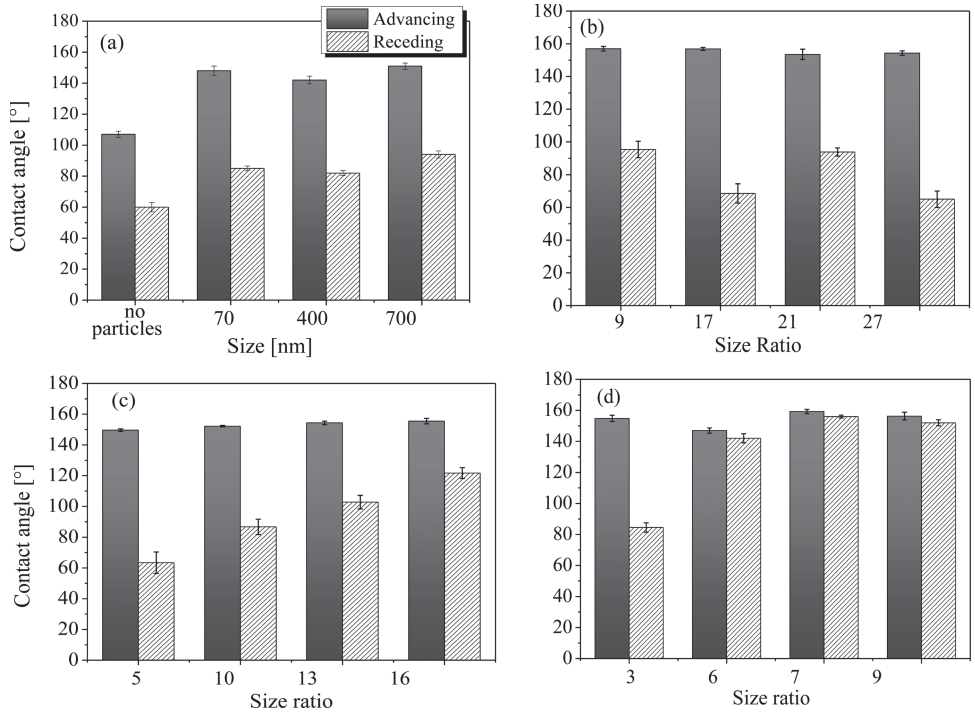

Figure 3. Dynamic contact angles on films prepared with (a) no particles and single-scale large size (LS) particles only, and with raspberry particles with different small feature particles (SS): (b) 15 nm, (c) 25 nm and (d) 45 nm. Size ratio (*r*) given by LS/SS.

films made from large silica particles, LS ~ 500 nm, which did not improve in performance even after a multi-scale roughness was introduced by several LBL depositions.

In clear contrast, the films prepared from raspberry particles showed different wetting behavior, dependent on both the scale of the small features constituting the raspberry (SS) and the size ratio (*r*) (Figure 3b to d). All the films prepared exhibited advancing CA above 150°. The noticeable discrepancy between the wettability behavior of the films lies, however, in the receding contact angle and therefore in the CAH. The films made with raspberry particles comprising 15 nm SS all exhibit a high hysteresis, independently of the features size and size ratio of the particles (Figure 3b). The CAH of the films with raspberries with 25 nm SS particles is, however, decreasing with the increasing ratio, from 93° for a $r = 5$ down to 33° for a $r = 16$ (Figure 3c). Finally, the films made of raspberry particles with 45 nm SS features exhibit very low hysteresis (~5°) if the size ratio is ≥6, but a much higher CAH was observed for lower ratios, i.e., almost 80° for $r = 3$ (Figure 3d).

These results demonstrate the importance of the scale of the raspberry particle's features on the wetting properties of the films. While the overall size or the size ratio of the raspberry particles does not seem to affect the advancing CA, the simple presence of small features (SS particles with a few tens of nanometer) on the films allows reaching higher advancing CA as compared to films made with large features only (LS particles with a few hundreds of nanometers). This result was also previously reported by others.[16] The hysteresis on the surface is, however, strongly linked to both the size of the small features forming the raspberry particles, as well as the size ratio between the small and large features. In fact, our results experimentally confirm the simulation study based on a Gibbs energy model of liquid droplets lying on dual-scale raspberry structured surfaces[28] which predicted that below a ratio of ca. 5, the superhydrophobic state as defined by Cassie-Baxter[29] is no longer viable. They, however, bring an additional scale restriction to the validity of the model, i.e., a minimal size for the small scale features.

4. Time-dependent Wettability of Films Made from Raspberry Nanoparticles When Exposed to Different Atmospheres

To investigate the wetting of our dual-structured surfaces, we performed time-dependent experiments to assess the stability of the wetting behavior. A water droplet of about 20 µL was deposited on the film made from raspberry particles with $r = 16$ (LS-400/SS-25 nm) and rested for 20 minutes after which, the receding contact angle was measured again (see **Figure 4**a). Every measurement was performed successively on the same position of the surface. The initial hysteresis, of approximately 30°, increases gradually with the resting time of the droplet, up to a maximum of 89° in 20 minutes. Interestingly, when a new droplet was immediately deposited at the exact same position and the receding angle measured directly, the hysteresis was back to its initial value (Figure 4a). The same experiment was performed for the other films made with raspberries containing SS-25 nm features (Figure 4b). Within the same time-frame, a similar (increased) CAH were observed for all the films.

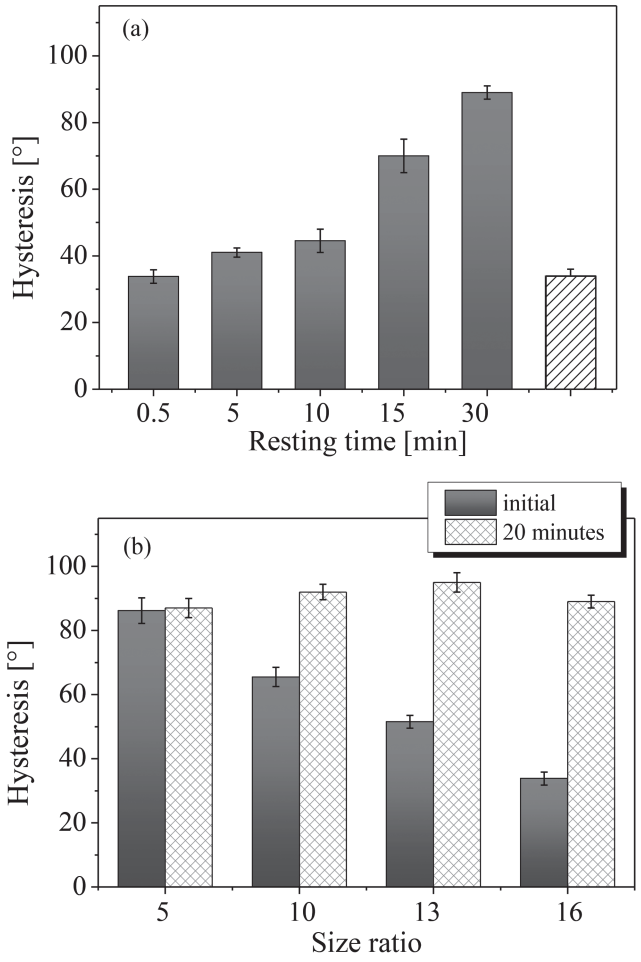

Figure 4. (a) Contact angle hysteresis of a 20 μL water droplet measured on a film made of raspberry particles composed of SS-25 nm and LS-400 nm particles with various resting times. The striped bar corresponds to the hysteresis measured in the same spot, with a fresh water droplet, immediately after the 30 minutes resting time and allowing 30 seconds exposure to air. (b) Initial contact angle hysteresis and after 20 minutes of resting time of the water droplet on films originated from raspberry particles with SS-25 nm small features.

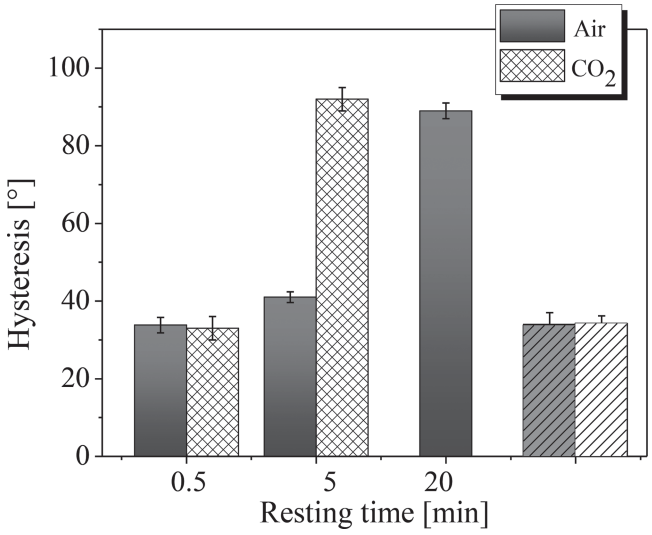

Figure 5. Contact angle hysteresis of a droplet (50 μL) of pure water under air and CO_2 atmosphere, measured on the film made of raspberry particles composed of SS-25 nm and LS-400 nm particles, versus water droplet resting time. The striped bar corresponds to the hysteresis measured in the same spot, with a fresh water droplet, immediately after the 20 minutes resting time and allowing 30 seconds exposure to air or CO_2 atmosphere, respectively.

These results clearly demonstrate a time-dependent evolution of the wetting state on the raspberry films. To investigate the origin of this wetting behavior, the time-dependent experiment was repeated but using a droplet of pure water under CO_2 saturated atmosphere which rested on the surface of the same film with $r = 16$ for a certain time-period. Interestingly, after 5 minutes only, the CAH reached the same value obtained for 20 minutes of resting time of the water droplet in air atmosphere (**Figure 5**). It should be noticed that in this case, the hysteresis also recovered the initial value when exactly the same surface spot was measured, directly after the experiment. This time-dependent wetting behavior could have two possible explanations; either the surface chemical groups react/rearrange in the presence of water or the air entrapped into the raspberry features is dissolving in time into the water droplet. Considering the first hypothesis, if the surface chemical groups react with water, we would expect the hysteresis to remain high after long exposure to water and that the initial value would not be fully retrieved. Furthermore, any possible surface rearrangements at the molecular level are expected to happen in much shorter time-frames than the resting times used, not exceeding approximately a few tens of seconds.[30] Hence, surface reactivity or rearrangements is an unlikely scenario. The second possibility, however, is much more feasible in view of the wettability tests made with different environments. By changing the atmosphere around the surface, i.e., by replacing air by carbon dioxide (CO_2), the rate of dissolution of the gas entrapped in the small features of the raspberry particles into the water droplet increased, leading to a faster change in the CAH in a CO_2 saturated atmosphere. In fact, similar phenomena of entrapped air dissolving into water were reported in the literature[31–33] but referring to structures fully immersed in water.

Considering wetting on rough surfaces, two main regimes have been recurrently discussed in the literature. In the regime described by Wenzel[34] the water droplet wets all the areas between the large asperities of the surface and the contact angle is given by,

$$\cos\theta_w = \rho\cos\theta \quad (1)$$

where θ_w is the Wenzel apparent contact angle on a rough surface, θ is the Young's contact angle on a similar smooth surface, and ρ is the surface roughness factor, defined as the ratio of the real wetted area to the projected (ideally smooth) wetted area of the solid surface ($\rho = 1$ for a perfectly smooth surface, and $\rho > 1$ for a rough one). For some particular rough surfaces, however, a significant volume of air can be entrapped between the water droplet and the surface asperities. For this regime, Cassie and Baxter[29] proposed a model taking into account the air fraction entrapped in the structure as given by,

$$\cos\theta_c = \varphi\cos\theta - (1-\varphi) \quad (2)$$

where θ_c is the Cassie-Baxter apparent contact angle, φ the fraction of surface that is wetted and $(1-\varphi)$ the fraction of surface covered with air. The results we obtained with the raspberry films indicate that the Cassie-Baxter state is only viable at certain sizes and size ratios, where it is a metastable state, i.e., the system can evolve to a different regime which will be more stable, hence, a transition from the Cassie-Baxter to the Wenzel state can occur. A simple criterion for this transition, valid for surfaces described by a (average) wavelength λ and (average) amplitude a, states that the transition can take place when $a > (\lambda/2\pi)\tan\theta$, where θ is the intrinsic contact angle.[35] Using for the intrinsic contact value, our experimental value of $\theta \cong 108°$ (Figure 3a, no particles), the critical amplitude calculated is about 50 nm. In order to assess whether this transition is relevant for our surfaces, we measured the surface roughness profile of the films made from raspberries particles with $r = 21$ (SS-15 nm and LS-315 nm) by Atomic Force Microscopy (AFM). The average wavelength was experimentally estimated (see Figure SI-3 for typical examples of AFM images and roughness profile used) to be about 0.1 μm, while the average and maximum amplitude are estimated to be ~30 nm and ~160 nm, respectively. Hence, considering these values, the roughness of the probed surface allows for a spontaneous transition between the Cassie-Baxter and Wenzel state. The rather large CAH observed for this raspberry film (~ 55°, from Figure 3b) is consistent with this assumption. It should be noted that the criterion mentioned is designed for a simple surface without any sharp transitions and having a single wavelength. Neither the one nor the other premise is valid for the present surfaces. Nevertheless, this estimate indicates that for the combination of particle feature sizes considered, the transition conditions are approximately met. Furthermore, our observation of time-dependent hysteresis on the studied surface provides additional evidence of the metastability of the Cassie-Baxter state. The air entrapped in the roughness features under the water droplet may largely dissolve into the liquid phase, leading to a higher water adhesion state. As the dissolution of entrapped air proceeds, the contact area between the water droplet and the asperities of the surface increases, until the surface is significantly wet. The small features present on the raspberry films further help to pin the water droplet, leading to sequentially higher adhesion of the water to the surface. Note that for all our coatings (shown in Figure 1), we observed the transition from the Cassie-Baxter to the Wenzel state. This may be due to the fact that in all the cases not enough air could be entrapped to maintain a stable Cassie-Baxter regime. Other researchers investigated the effect of water intrusion into micrometer-sized features due to the droplet weight, either by varying the volume of the droplet[36] or by applying pressure onto it.[37,38] In our study, no difference was observed in the hysteresis when 20 or 50 μL droplets were used. Finally, it should be pointed out that our approach has a valuable asset to offer for this wettability study. Using the different size scale and size ratio of the raspberries prepared, we made a set of monolayer-films with a well-defined dual-scale morphology available, which allows entrapping a controlled and 'limited' volume of air on the surface. To the best of our knowledge, this is the first time that the time-dependent diffusion of air entrapped into a Cassie-Baxter state and the associated implications about the wettability and the stability of that state, is described for experimentally prepared well-defined and hierarchically structured films.

5. Conclusions

In summary, by employing raspberry silica-silica particles of various sizes and size ratios we extended the existing knowledge on the fundamentals of wetting phenomena. While the advancing water contact angle appears not to depend on the size or size ratio of the particles used, the hysteresis on the surface is, however, strongly linked to both parameters. To reach superhydrophobicity, defined by high contact angle (>150°) and low CAH, the smaller features of the dual scale roughness should be at least 25 nm in diameter. For individual features of 45 nm, a ratio (given by large over small features) larger than 5 is necessary. In addition, the transition between the Cassie-Baxter state and the Wenzel regime could be observed by letting a water droplet rest on the surface and measuring its time evolution. The dissolution of the air entrapped below the droplet in the asperities of the surface was shown to be responsible for this transition, leading to higher hysteresis, and hence higher water adhesion to the surface. These new insights into the wetting properties of the surface should be taken into account in the specifications for designing rough surfaces for superhydrophobic surfaces, which show properties such as self-cleaning, low-adhesion, anti-icing or reduced-drag, and can find applications on solar panels, green-houses, sky-scrapers, airplanes, boats, clothes, microfluidics, mobiles and many other electronic devices.

6. Experimental Section

Materials: Tetraethyl orthosilicate (TEOS, 99%), aminopropyl triethoxysilane (APTES, 98%) and aqueous ammonia solution (25%) were obtained from Merck and glycidoxypropyl trimethoxysilane (GPS, 98%) from Aldrich. L-lysine (reagent grade) was purchased from Fluka. Trimethylolpropane triglycidyl ether (TPTGE, technical grade) and monoglycidyl ether terminated polydimethylsiloxane (M_w = 5000) were obtained from Aldrich. Jeffamine D-230 (a polyoxypropylene diamine) was purchased from Huntsman and aminopropyl terminated polydimethylsiloxane (DMS-A15, M_w = 3000) was obtained from ABCR. Ethanol, propanol and toluene were purchased from Biosolve (p.a. grade). All solvents were of p.a. grade and the chemicals were used as received without further purification.

The diafiltration membranes (50 and 500 kDa, Polysulfone) were purchased from SpectrumLabs and flushed with water or preferred buffer in order to remove hydrogen peroxide prior to use.

Preparation of Silica Nanoparticles: The silica nanoparticles were prepared with different sizes and size ratios, according to the procedures described in the literature.[25,26] All raspberry particles employed for preparing the films are lysine raspberry particles, i.e., obtained by combining large (LS) Stöber[25] made particles and small (SS) lysine[26] made particles.

Epoxy-modified Silica Nanoparticles Prepared via the Stöber[25] method, SS >30 nm: Stöber silica particles with sizes ranging from 60 to 500 nm in diameter were prepared by adding TEOS (6 mL) to a closed-round bottom flask equipped with a condenser and containing aqueous ammonia solution (15 mL) and alcohol solvent (200 mL). The reaction was performed under magnetic stirring (270 rpm) for 5 h. The size of the particles is tuned by varying the temperature (from 5 to 60 °C, the lower

the temperature, the larger the particles) and the solvent (propanol is used for larger particles). After washing and drying the silica powders, the particles (1.5 g) were redispersed into 50 mL toluene and GPS (0.3 mL) in 5 mL toluene was added dropwise to the silica suspension. The reaction was carried out at 50 °C under N_2 atmosphere for 24 hours, after which the particles were separated and dried.

Amino-modified Silica Nanoparticles Prepared via the Amino-Acids[26] *method, SS ≤ 50 nm*: Silica particles with diameter below 50 nm were prepared according to the lysine mediated approach; reagent grade lysine (0.1 g) was dissolved in deionized water (100 mL) under magnetic stirring. Thereafter, TEOS (6 mL) was added to the water-lysine solution. The reaction was carried out at 60 °C for 24 h under magnetic stirring (270 rpm). Additional amount of TEOS could be added to the reaction vessel at 60 °C to grow the silica particles to larger sizes. 2 mL of an aqueous solution of APTES (35 µL in 20 mL water) was slowly added into 10 mL of the as-prepared suspension (1.5 mL/h); the reaction was carried out for 16 hours at 60 °C, after which the suspension was diafiltered against water to remove unreacted APTES and excess lysine.

Silica Raspberry Nanoparticles: The raspberry silica particles were prepared by modifying slightly a method reported before[17] by slowly adding the epoxy-modified particles suspended in ethanol (0.2 wt%) into a suspension of amine-modified particles in water (0.02 wt%) under magnetic stirring at room temperature for 16 hours.

Preparation of Silica Raspberry Nanoparticle Layers onto Epoxy Films

Epoxy-amine Films with Dual-size Roughness: A conventional epoxy-amine polymer film with the epoxy in 10% excess was applied on an aluminum substrate that was previously thoroughly cleaned by successively technical ethanol, acetone and toluene and dried with pulsed air. Then, a mixture of TPTGE (0.44 g) and Jeffamine D-230 (0.24 g) dissolved in toluene (1 mL) was applied onto the aluminum substrate with a doctor blade applicator driven by a Master Coat film apparatus (wet film thickness of 30 µm, 5 $mm.s^{-1}$) and cured at 75 °C for 5 hours. Next, raspberry silica particles were suspended in ethanol (0.040 g in 1 mL, 4.8 wt%). The suspension was then spin-coated (Laurell WS-650–23NPP-LITE Spin Coater, 1000 rpm, 30 seconds) on the epoxy film and the film was left to react at 75 °C for 16 hours. After cooling, the film was dipped in toluene and placed in a sonicator bath for 1 minute to remove unconnected particles, and dried with pulsed air at room temperature.

Hydrophobization Procedure for the Dual-size Roughened Films: The films were rendered hydrophobic by grafting polydimethylsiloxane (PDMS) onto the double-structured film containing raspberry particles. The film was first reacted with amine-end-capped PDMS by applying a drop of DMS A-15 onto the film and placing it at 80 °C for 4 h to ensure that any unreacted epoxy groups, from the epoxy-amine film or from the epoxy modified particles from the raspberry synthesis, were provided with amine terminated PDMS. The film was then thoroughly rinsed with toluene to remove unreacted DMS A-15 and dried with pulsed air. Next, the film was reacted with monoglycidyl ether terminated PDMS by depositing a drop onto the surface of the film and placed at 80 °C for 4 hours. Finally, the film was carefully rinsed with toluene and dried with pulsed air.

7. Methods

Scanning Electron Microscopy (SEM): SEM was performed using a FEI Quanta 3D FEG with a field emission gun as electron source at an acceleration voltage of 5 to 15 kV. Before scanning, the samples were prepared on aluminum stubs by evaporation of a droplet of nanoparticles suspension and sputter-coated with a conductive metal to enhance the imaging quality. Chromium (Cr) was the material of choice since its grain size is below the resolution of the SEM; the Cr layer was deposited with a Turbo Sputter Coater K575X dual for 40 seconds at 100 mA.

Contact Angle (CA) Measurements: CA measurements were performed on a Dataphysics OCA 30 using ultrapure water as probe liquid. The dynamic contact angles were determined by using the ARCA (Advancing Receding Contact Angle) function of the OCA software that controls the addition and withdrawal of water to a deposited drop using a microsyringe kept inside the drop Typically, a 0.5 µL droplet was deposited on the surface and its volume was increased to 15 µL within 30 seconds, after which the water was withdrawn from the droplet, to determine the advancing and receding contact angles, respectively (see Figure SI-4). For the time-dependent experiments, the receding contact angle was determined as a function of the time the droplet was left to rest on the surface. Typically, a 50 µL droplet was deposited on the surface and the water was sucked out directly, corresponding to the 0.5 min receding time, and leaving a dry surface. Immediately after, a new 50 µL droplet was placed on exactly the same position at the surface and let to rest for 5 minutes, after which the water was removed from the drop and the 5 min receding angle determined. The operation was repeated for various periods of time, up to 30 minutes resting time for the water drop. The evaporation of water from the droplet was negligible, as compared to the initial volume, hence ignored. Finally, the last measurement consisted in measuring the receding angle of a droplet that was once again deposited at the exactly same position as before, without extra resting time. For some of the measurements, probe liquids other than pure water were used; in that case, a peristaltic pump was used to control the slow addition and withdrawal of liquid from the surface. In addition, a temperature control chamber was used to work under CO_2 atmosphere; the samples were placed in the chamber that was flushed with CO_2 for 6 hours. The measurements were then performed at 20 °C without opening the chamber. All the contact angles were determined by averaging the values measured at least at three different points on each sample and the error bars give the corresponding sample standard deviation.

Transmission Electron Microscopy (TEM): TEM imaging was performed with a FEI Tecnai 20 TEM (type Sphera, LaB_6 filament, 200 kV, 1k x 1k Gatan CCD camera). The samples were prepared by allowing 5 µL of the suspension to dry on a 200 mesh Cu grid with continuous carbon film (Agar Scientific).

Atomic Force Microscopy (AFM): AFM characterization was performed with a NT-MDT NTegra Aura in semi-contact (tapping) topography mode using silicon NSG11 cantilevers (NT-MDT) with a typical spring constant of 5.5 N/m, resonance frequency of 150 KHz and tip radius of 10 nm. The scanning velocity was ~ 2 µm/s employing 512 × 512 images.

Supporting Information

Supporting Information is available from the Wiley Online Library or from the author.

Acknowledgements

This study was partly supported by DSM Ahead Performance Materials B.V., The Netherlands.

Received: January 13, 2014
Revised: March 6, 2014
Published online: July 14, 2014

[1] X. M. Li, D. Reinhoudt, M. Crego-Calama, *Chem. Soc. Rev.* **2007**, *36*, 1350.
[2] M. Nosonovsky, B. Bhushan, *Curr. Opin. Colloid Interf.* **2009**, *14*, 270.
[3] P. Roach, N. J. Shirtcliffe, M. I. Newton, *Soft Matter* **2008**, *4*, 224.
[4] X. Zhang, F. Shi, J. Niu, Y. G. Jiang, Z. Q. Wang, *J. Mater. Chem.* **2008**, *18*, 621.
[5] W. Barthlott, C. Neinhuis, *Planta* **1997**, *202*, 1.
[6] J. Wang, H. Chen, T. Sui, A. Li, D. Chen, *Plant Sci.* **2009**, *176*, 687.
[7] B. T. Qian, Z. Q. Shen, *Langmuir* **2005**, *21*, 9007.
[8] E. Hosono, S. Fujihara, I. Honma, H. S. Zhou, *J. Am. Chem. Soc.* **2005**, *127*, 13458.

[9] Y. Li, X. J. Huang, S. H. Heo, C. C. Li, Y. K. Choi, W. P. Cai, S. O. Cho, *Langmuir* **2007**, *23*, 2169.
[10] S. H. Sajadinia, F. Sharif, *J. Coll. Interf. Sci.* **2010**, *344*, 575.
[11] E. Bittoun, A. Marmur, *Langmuir* **2012**, *28*, 13933.
[12] N. A. Patankar, *Langmuir* **2004**, *20*, 8209.
[13] L. Mammen, X. Deng, M. Untch, D. Vijayshankar, P. Papadopoulos, R. Berger, E. Riccardi, F. Leroy, D. Vollmer, *Langmuir* **2012**, *28*, 15005.
[14] Y. W. Su, B. H. Ji, K. Zhang, H. J. Gao, Y. G. Huang, K. Hwang, *Langmuir* **2010**, *26*, 4984.
[15] H. H. Liu, H. Y. Zhang, W. Li, *Langmuir* **2011**, *27*, 6260.
[16] H. Teisala, M. Tuominen, M. Aromaa, M. Stepien, J. M. Mäkelä, J. J. Saarinen, M. Toivakka, J. Kuusipalo, *Langmuir* **2012**, *28*, 3138.
[17] W. Ming, D. Wu, R. A. T. M. van Benthem, G. de With, *Nano Lett.* **2005**, *5*, 2298.
[18] N. Puretskiy, L. Ionov, *Langmuir* **2011**, *27*, 3006.
[19] H. J. Tsai, Y.-L. Lee, *Langmuir* **2007**, *23*, 12687.
[20] Z. Qian, Z. Zhang, L. Song, H. Liu, *J. Mater. Chem.* **2009**, *19*, 1297.
[21] D. Z. Xu, M. Z. Wang, X. W. Ge, M. H. W. Lam, X. P. Ge, *J. Mater. Chem.* **2012**, *22*, 5784.
[22] X. Fan, L. F. Zheng, J. Cheng, S. P. Xu, X. F. Wen, Z. Q. Cai, P. H. Pi, Z. R. Yang, *Surf. Coat. Tech.* **2012**, *213*, 90.
[23] M. D'Acunzi, L. Mammen, M. Singh, X. Deng, M. Roth, G. K. Auernhammer, H. J. Butt, D. Vollmer, *Faraday Discuss.* **2010**, *146*, 35.
[24] X. Y. Li, J. H. He, *ACS Appl. Mater. Interf.* **2012**, *4*, 2204.
[25] W. Stöber, A. Fink, E. Bohn, *J. Coll. Interf. Sci.* **1968**, *26*, 62.
[26] T. Yokoi, Y. Sakamoto, O. Terasaki, Y. Kubota, T. Okubo, T. Tatsumi, *J. Am. Chem. Soc.* **2006**, *128*, 13664.
[27] D. Wu, *PhD Thesis, Nature-inspired Superlyophobic Surfaces*, Eindhoven University of Technology, 2007.
[28] R. J. Vrancken, *PhD Thesis, Controlling Drop Morphology*, Eindhoven University of Technology, The Netherlands 2012.
[29] A. Cassie, S. Baxter, *Trans. Faraday Soc.* **1944**, *40*, 546.
[30] D. Y. Kwok, A. W. Neumann, *Adv. Colloid Interf. Sci.* **1999**, *81*, 167.
[31] M. S. Bobji, S. V. Kumar, A. Asthana, R. N. Govardhan, *Langmuir* **2009**, *25*, 12120.
[32] R. Poetes, K. Holtzmann, K. Franze, U. Steiner, *Phys. Rev. Lett.* **2010**, *105*, 1661041.
[33] M. A. Samaha, H. V. Tafreshi, M. Gad-el-Hak, *Langmuir* **2012**, *28*, 9759.
[34] R. N. Wenzel, *J. Phys. Colloid Chem.* **1949**, *53*, 1466.
[35] R. E. Johnson, R. H. Dettre, Contact Angle, Wettability and Adhesion, *Adv. Chem. 43*, *Am. Chem. Soc.* Washington DC **1964**.
[36] Z. Yoshimitsu, A. Nakajima, T. Watanabe, K. Hashimoto, *Langmuir* **2002**, *18*, 5818.
[37] J. Bico, C. Marzolin, D. Quere, *Europhys. Lett.* **1999**, *47*, 220.
[38] A. Lafuma, D. Quere, *Nat. Mater.* **2003**, *2*, 457.